Generalized SAFT-DFT/DMT Model for the Thermodynamic, Interfacial, and Transport Properties of Associating Fluids: Application for *n*-Alkanols

S. B. Kiselev* and J. F. Ely

Chemical Engineering Department, Colorado School of Mines, Golden, Colorado 80401-1887

I. M. Abdulagatov and M. L. Huber

Physical and Chemical Properties Division, National Institute of Standards and Technology, Boulder, Colorado 80305

We have developed a "global" crossover (GC) statistical associating fluid theory (SAFT) equation of state (EOS) for associating fluids that incorporates nonanalytic scaling laws in the critical region and in the limit of low densities, $\rho \rightarrow 0$, is transformed into the ideal-gas equation EOS. Unlike the crossover SAFT EOS developed earlier, the new GC SAFT EOS contains a so-called kernel term and reproduces the asymptotic scaling behavior of the isochoric heat capacity in the one- and two-phase regions. In addition, we develop on the basis of the density functional theory (DFT) a GC SAFT-DFT model for the surface tension. In the second step, using the GC SAFT EOS and the decoupled-mode theory (DMT), we have developed a generalized GC SAFT-DMT model for transport coefficients that reproduces the singular behavior of the thermal conductivity of pure fluids in the critical region. Unlike the DMT model based on the asymptotic crossover EOS, the GC SAFT-DMT model is valid in the entire fluid state region at $T \geq T_b$ (where T_b is the binodal temperature), and at $\rho \rightarrow 0$ reproduces the dilute gas contributions for the transport coefficients. A comparison was made with experimental data for methanol, ethanol, and higher *n*-alkanols. For *n*-alkanols, the GC SAFT-DFT/DMT model contains the same number of the adjustable parameters as the original classical SAFT EOS but reproduces with high accuracy the *PVT*, VLE, isochoric, and isobaric specific heats, surface tension, and thermal conductivity data close to and far from the critical point.

1. Introduction

In associating fluids such as *n*-alkanols, strong attractive interactions between molecules result in the formation of molecular clusters that have considerable effect on the thermodynamic and structural properties of the species. Due to their high polarity and strong self-association, *n*-alkanols, and in particular methanol, are complex fluids that are extremely challenging for both experimental and theoretical study. Experiments dealing with the thermodynamic and transport properties over a wide temperature range of such a thermally labile species as associating fluids are often hindered by chemical reactions, including decomposition. Therefore, extrapolation of different empirical and semi-empirical multi-parameter equations of state (EOS) for *n*-alkanols in the range of conditions where no experimental data were used for their optimization is often unreliable and in general is not recommended. On the other hand, molecular-based equations of state, such as statistical associating fluid theory (SAFT), employ equations that have been developed as an alternative to empirical EOS for associating liquids. In its original[1−3] and modified[4−8] form, SAFT cannot reproduce the critical parameters T_c, P_c, and ρ_c simultaneously and is therefore incapable of reproducing different thermodynamic properties such as vapor−liquid equilibria (VLE), *PVT*, densities, specific heats, enthalpies, and excess properties in the gas and liquid phases simultaneously with the same set of the system-dependent parameters. In addition, all of these analytical EOS fail to reproduce the nonanalytical, singular behavior of fluids in the critical region, caused by long-scale fluctuations in density.

A general procedure for incorporating long-range density fluctuations into any classical−analytical equation was proposed by Kiselev[9] based on renormalization-group theory This procedure has been successfully applied to the SAFT,[10−12] SAFT-BACK,[13] and SAFT-VR[14,15] EOS. In all cases, this method produces a thermodynamically self-consistent and accurate crossover EOS near to and far from the critical points of pure fluids. Recently, in combination with the generalized crossover density functional (DFT) and decoupled mode theory (DMT), this procedure has been also extended to the interfacial[14,16] and transport[17] properties of pure fluids.

In this paper, we continue a study initiated in our previous works for cubic[16,17] and SAFT EOS.[11] First, we have developed a "global" crossover (GC) SAFT EOS for methanol, ethanol, and higher *n*-alkanols, which unlike the crossover SAFT EOS developed earlier[11] contains a so-called kernel term[18] and reproduces the asymptotic scaling behavior of the isochoric heat capacity in the critical region. Second, on the basis of the GC SAFT equation and the density functional theory, we developed a generalized GC SAFT-DFT model for surface tension. Combining the GC SAFT equation with the

* To whom correspondence should be addressed: Phone: (303)273-3190. Fax: (303)273-3730. E-mail: skiselev@mines.edu.

10.1021/ie050010e CCC: $30.25
Published on Web 07/02/2005

crossover decoupled mode theory, we have also developed a GC SAFT-DMT model for the transport properties and have compared this model with experimental thermal conductivity and thermal diffusivity data for methanol and ethanol.

We proceed as follows. In section 2, we describe a general procedure for transforming the analytical SAFT equation into the crossover form and obtain a GC SAFT EOS in closed analytical form. In section 3, we develop a GC SAFT EOS for *n*-alkanols and provide an extensive comparison with experimental data. In section 4, we present a GC SAFT-DFT model for the surface tension. A generalized crossover SAFT-DMT model for the transport properties is considered in section 5. Our results are summarized and discussed in section 6.

2. Thermodynamic Model

2.1. Classical SAFT Equation. In this work, for a reference classical SAFT EOS we adopt the model developed by Huang and Radosz.[4,5] The molar residual Helmholtz energy (A^{res}) in this model consists of three terms:

$$\frac{A^{\mathrm{res}}}{RT} = a^{\mathrm{res}} = a^{\mathrm{seg}} + a^{\mathrm{chain}} + a^{\mathrm{assoc}} \tag{1}$$

where a^{seg} is the Helmholtz energy due to segment−segment interactions, a^{chain} is the incremental Helmholtz energy due to chain formation, and a^{assoc} is the incremental Helmholtz energy due to association.

The segment contribution is given by[4,5]

$$a^{\mathrm{seg}} = m(a_{\mathrm{o}}^{\mathrm{hs}} + a_{\mathrm{o}}^{\mathrm{disp}}) \tag{2}$$

where m is the number of segments per molecule and $a_{\mathrm{o}}^{\mathrm{hs}}$ is the Helmholtz energy of hard-sphere fluids per segment given by Carnahan and Starling:[19]

$$a_{\mathrm{o}}^{\mathrm{hs}} = \frac{4\eta - 3\eta^2}{(1-\eta)^2} \tag{3}$$

where $\eta = \pi/6 N_{\mathrm{A}} \rho m d^3$ is the reduced density, and

$$d = \sigma\left[1 - C\exp\left(\frac{-3u^{\mathrm{o}}}{k_{\mathrm{B}}T}\right)\right] \tag{4}$$

is the temperature-dependent segment diameter. In eqs 1−4, R is the gas constant; N_{A} is Avogadro's number; ρ is the molar density; σ is the center-to-center distance between two segments, at which the pair potential of the real fluid is zero (the temperature-independent segment diameter); k_{B} is the Boltzmann constant; $C = 0.12$ for all fluids in this work; and u^{o} is the temperature-independent well depth of the square-well potential. The temperature-independent segment diameter (σ) is related to the temperature-independent segment molar volume in a close-packed arrangement defined per mole of segments:

$$v^{00} = \frac{\pi}{6}\frac{N_{\mathrm{A}}}{\tau}\sigma^3 \tag{5}$$

where $\tau = \sqrt{2}\pi/6$. The dispersion part in eq 2 ($a_{\mathrm{o}}^{\mathrm{disp}}$) is given by the Chen−Kreglewski expression:[20]

$$a_{\mathrm{o}}^{\mathrm{disp}} = \sum_i \sum_j D_{ij}\left[\frac{u}{k_{\mathrm{B}}T}\right]^i\left[\frac{\eta}{\tau}\right]^j \tag{6}$$

where the coefficients D_{ij} are universal constants; u is the temperature-dependent well depth defined as

$$u = u^{\mathrm{o}}\left(1 + \frac{\epsilon}{k_{\mathrm{B}}T}\right) \tag{7}$$

and the parameter ϵ/k, which in general is related to the critical temperature and Pitzer's acentric factor ω, for SAFT molecules was set[4] to $\epsilon/k_{\mathrm{B}} = 10$.

The chain contribution (a^{chain}) in eq 1 is given by

$$a^{\mathrm{chain}} = -(m-1)\ln g^{\mathrm{hs}}(d) \tag{8}$$

where $g^{\mathrm{hs}}(d) = (2-\eta)/2(1-\eta)^3$ is the radial distribution function of the hard-sphere fluid at contact.

The association contribution (a^{assoc}) in eq 1 is given by[4,5]

$$a^{\mathrm{assoc}} = \sum_{A\in\Gamma}\left(\ln X^{\mathrm{A}} - \frac{X^{\mathrm{A}}}{2}\right) + \frac{n(\Gamma)}{2} \tag{9}$$

where $n(\Gamma)$ is the number of association sites on the molecule and X^{A} is the fraction of molecules that are not bonded at site A. The expression for X^{A} is written in the form

$$X^{\mathrm{A}} = (1 + N_{\mathrm{A}}\rho\sum_{B\in\Gamma} X^{\mathrm{B}}\Delta^{\mathrm{AB}})^{-1} \tag{10}$$

where Δ^{AB} is the association strength given by

$$\Delta^{\mathrm{AB}} = \sigma^3\kappa^{\mathrm{AB}}\left[\exp\left(\frac{\epsilon^{\mathrm{AB}}}{k_{\mathrm{B}}T}\right) - 1\right]g^{\mathrm{hs}}(d) \tag{11}$$

where ϵ^{AB} is the well depth of the site−site potential and $\sigma^3\kappa^{\mathrm{AB}}$ is a measure of the volume available for bonding. To obtain specific expressions for a^{assoc} and X^{A}, one has to hypothesize the number of association sites and make simplifying approximations for the association strength of site−site interactions. Here, similar to our previous work,[11] *n*-alkanols are modeled as associating chain molecules with two association sites (i.e., model 2B).[4]

The total number of SAFT parameters for associating fluids is five; namely, the segment number (m), the segment volume (v^{00} or σ), the well depth of the segment−segment potential (u^0), site−site (ϵ^{AB}) interaction, and the volume bonding parameter (κ^{AB}). The classical critical molar density and temperature (i.e., $\rho_{0\mathrm{c}}$ and $T_{0\mathrm{c}}$) are obtained by solving the criticality conditions:

$$\left(\frac{\partial P}{\partial \rho}\right)_{T_{0\mathrm{c}}} = \left(\frac{\partial^2 P}{\partial \rho^2}\right)_{T_{0\mathrm{c}}} = 0 \tag{12}$$

where P is the pressure. Once $\rho_{0\mathrm{c}}$ and $T_{0\mathrm{c}}$ are known, the critical pressure $P_{0\mathrm{c}}$ can be also obtained.

2.2. Crossover SAFT Equation. To obtain a GC EOS, which in the critical region reproduces all known scaling laws and in the limit of low densities is reduced to the ideal-gas EOS, we follow the crossover approach developed by Kiselev.[9] Following this approach, we first

represent the dimensionless Helmholtz free energy $a(T, v) = A(T, v)/RT$ in the form

$$a(T, v) = \Delta a(\Delta T, \Delta v) + a_{bg}(T, v) \quad (13)$$

where the critical part of the dimensionless Helmholtz free energy

$$\Delta a(\Delta T, \Delta v) = a^{res}(\Delta T, \Delta v) - a_o^{res}(\Delta T) + \bar{P}_0(\Delta T)\Delta v - \ln(\Delta v + 1) \quad (14)$$

and the background contribution is given by

$$a_{bg}(T, v) = a_o^{res}(T) + a^{id}(T) - \bar{P}_0(T)\Delta v \quad (15)$$

In eqs 14 and 15, $v = 1/\rho$ is a molar volume, $\Delta T = T/T_{0c} - 1$ and $\Delta v = v/v_{0c} - 1$ are dimensionless distances from the classical critical temperature (T_{0c}) and molar volume (v_{0c}), respectively; $\bar{P}_0(T) = P_0(T, v_{0c})v_{0c}/RT$ is the dimensionless pressure; $a_o^{res}(T) = a^{res}(T, v_{0c})$ is the dimensionless residual part of the Helmholtz energy along the critical isochore ($v = v_{0c}$); and $a^{id}(T)$ is the dimensionless temperature-dependent ideal-gas Helmholtz free energy.

In the second step, we replace the classical values of ΔT and Δv in the critical part $\Delta a(\Delta T, \Delta v)$ with the renormalized values:[11,18]

$$\bar{\tau} = \tau Y^{-\alpha/2\Delta_1} + (1 + \tau)\Delta T_c Y^{2(2-\alpha)/3\Delta_1} \quad (16)$$

$$\bar{\varphi} = \varphi Y^{(\gamma-2\beta)/4\Delta_1} + (1 + \varphi)\Delta v_c Y^{(2-\alpha)/2\Delta_1} \quad (17)$$

where $\alpha = 0.11$, $\beta = 0.325$, $\gamma = 2 - 2\beta - \alpha = 1.24$, and $\Delta_1 = 0.51$ are universal nonclassical critical exponents;[21,22] $\tau = T/T_c - 1$ is a dimensionless deviation of the temperature from the true critical temperature (T_c); $\varphi = v/v_c - 1$ is a dimensionless deviation of the molar volume from the true critical molar volume (v_c); $\Delta T_c = (T_c - T_{0c})/T_{0c} \ll 1$ and $\Delta v_c = (v_c - v_{0c})/v_{0c} \ll 1$ are dimensionless shifts of the critical temperature and volume, respectively; and $Y(\tau, \varphi)$ denotes a crossover function.

In this work, for the crossover function $Y(\tau, \varphi)$, we use a simple phenomenological expression obtained by Kiselev and co-workers:[9-11,18,23]

$$Y(q) = \left(\frac{q}{1 + q}\right)^{2\Delta_1} \quad (18)$$

where following our recent work for the generalized cubic EOS,[16,17] we find the renormalized distance to the critical point q from a solution of the crossover sine model (SM):

$$\left(q^2 - \frac{\tau}{Gi}\right)\left[1 - \frac{p^2}{4b^2}\left(1 - \frac{\tau}{q^2 Gi}\right)\right] = b^2\left\{\frac{\varphi[1 + v_1 \exp(-10\varphi)] + d_1\tau}{m_0 Gi^\beta}\right\}^2 Y^{1-2\beta/\Delta_1} \quad (19)$$

where the coefficients m_0, v_1, d_1, and the Ginzburg number (Gi) are the system-dependent parameters, while the universal parameters p^2 and b^2 can be set equal to the linear model (LM) parameter $p^2 = b^2 = b_{LM}^2 \cong 1.359$.[23] The crossover SM as given by eq 19 is physically equivalent to the crossover sine model developed earlier,[11,18,23] but with a different empirical term $\propto v_1 \exp(-10\varphi)$, which provides the physically obvious condition $Y = 1$ at the triple point of liquids.

Finally, a GC expression for the Helmholtz free energy can be written in the form

$$a(T, v) = \Delta a(\bar{\tau}, \bar{\varphi}) - K(\tau, \varphi) - \Delta v\bar{P}_0(T) + a_o^{res}(T) + a^{id}(T) \quad (20)$$

with the kernel term given by

$$K(\tau, \varphi) = \frac{1}{2}a_{20}\tau^2[Y^{-\alpha/\Delta_1}(\tau, \varphi) - 1] + \frac{1}{2}a_{21}\tau^2[Y^{-(\alpha-\Delta_1)/\Delta_1}(\tau, \varphi) - 1] \quad (21)$$

The coefficients a_{20} and a_{21} in eq 21 correspond to the asymptotic (A_0^+) and first Wegner correction (a_1^+), terms in the asymptotic expression[24] for the isochoric heat capacity $C_V = -T(\partial^2 A/\partial T^2)_\rho$ along the critical isochore at $\tau \to +0$:

$$C_V(\tau)/R = A_0^+|\tau|^{-\alpha}(1 + a_1^+|\tau|^{\Delta_1}) + B_{bg}^+(\tau) \quad (22)$$

where B_{bg}^+ is the background contribution above the critical temperature $T > T_c$. It is easy to demonstrate that in the generalized SAFT EOS with the kernel term as given by eq 21, the critical asymptotic and first correction amplitudes are given by

$$A_0^+ = \frac{(2 - \alpha)(1 - \alpha)}{2}a_{20}Gi^\alpha, \quad a_1^+ = \frac{(2 - \alpha + \Delta_1)(1 - \alpha + \Delta_1)}{(2 - \alpha)(1 - \alpha)}\frac{a_{21}}{a_{20}}Gi^{-\Delta_1} \quad (23)$$

The crossover EOS can be obtained by differentiation of eq 20 with respect to volume

$$P(v, T) = -RT\left(\frac{\partial a}{\partial v}\right) = \frac{RT}{v_{0c}}\left\{-\frac{v_{0c}}{v_c}\left[\left(\frac{\partial \Delta a}{\partial \varphi}\right)_T - \left(\frac{\partial K}{\partial \varphi}\right)_\tau\right] + \bar{P}_0(T)\right\} \quad (24)$$

The GC SAFT EOS as defined by eq 24 in addition to the classical SAFT parameters also contains the Ginzburg number (Gi), the rectilinear diameter (d_1), the sine model parameter (m_0), the crossover parameter (v_1), and the coefficients a_{20} and a_{21}; the last two parameters result specifically from the kernel term.

3. Thermodynamic Properties

The crossover SAFT EOS described above for associating fluids contains 11 system-dependent parameters and, as we have shown in our previous work on propan-1-ol,[18] is capable of describing the volumetric and caloric properties of one-component fluids with high accuracy. Unfortunately, this equation requires a substantial data set (including accurate VLE, PVT, C_p and C_v data) for the determination of optimal parameters; this prevents widespread use of the GC SAFT EOS for engineering calculations. In the present work, to reduce the number of adjustable parameters and make the GC SAFT EOS more predictive, we set the parameter m_0 to be a constant, $m_0 = 1.55$, while the parameters d_1 and v_1 are given as linear functions of the inverse Ginzburg number

$$v_1 = -2.15 \times 10^{-3} + 3.98 \times 10^{-4} Gi^{-1}, \quad d_1 = 4.443 - 0.143 Gi^{-1} \quad (25)$$

where the Ginzburg number in *n*-alkanols was found to be a simple linear function of the molar mass M_w:

$$Gi^{-1} = 3.40 + 0.227 M_w \quad (26)$$

In accordance with eq 23, we represent the parameter a_{20} in the kernel term in the form

$$a_{20} = \frac{2A_0^+}{Gi^{\alpha}}(2 - \alpha)(1 - \alpha) \quad (27)$$

where the asymptotic critical amplitude A_0^+ was set equal to the corresponding amplitude in the parametric crossover model[25]

$$A_0^+ = Z_c \frac{ak\gamma(\gamma - 1)}{2\alpha b_{LM}^2} \quad (28)$$

where the parameters a and k in eq 28 have been determined from the corresponding-state relations developed earlier by Kiselev et al.[26]

$$a = 15.645(1 + 19.220\Delta\omega), \quad k = 1.15(1 + 0.3327\Delta\omega^{0.895}) \quad (29)$$

where $\Delta\omega = \omega - 0.011$ is the difference between the acentric factor of the fluid of interest and the acentric factor of a reference system (methane in ref 26). In general, the second parameter in the kernel term (a_{21}) can be considered as an adjustable parameter in the GC SAFT EOS. However, according to the more rigorous renormalization-group theory calculations performed by Belyakov and Kiselev,[27] the ratio a_{21}/a_{20} in eq 23 is a system-independent constant. Therefore, in this work we set $a_{21} = -0.3a_{20}$, which appears to be a good approximation for the parameter a_{21} in *n*-alkanols. After this redefinition, only five adjustable parameters remain. If the actual critical temperature (T_c) and density (ρ_c) of the fluid of interest are known, the critical shifts (ΔT_c and Δv_c) and the critical compressibility ($Z_c = P_c/R\rho_c T_c$) are known as well, and the GC SAFT EOS for associating fluids contains the same number of adjustable parameters as the original SAFT EOS (i.e., m, v^{00}, u^o, ϵ^{AB}, and κ^{AB}). Otherwise, T_c and ρ_c should be considered as additional adjustable parameters of the model.

The first system that we consider here is methanol. Because of the high polarity and strong association between molecules, methanol is challenging to model; therefore, it is an interesting test for the GC SAFT EOS. The parameters m, v^{00}, u^o, ϵ^{AB}, and κ^{AB} for methanol have been found from a fit of the GC SAFT EOS to experimental one-phase region *PVT* data obtained by Zubarev et al.,[28] Finkelstein and Stiel,[29] Straty et al.,[30] and Bazaev et al.;[31] the liquid density data obtained by Machado and Street;[32] and the VLE data obtained by Ramsay and Young,[33] Donham,[34] Ambrose and Sprake,[35] and Abdulagatov et al.[36] Although the thermodynamic properties of methanol have been studied extensively by different researchers and by different experimental methods, as was shown by Abdulagatov et al.,[37] there is still a large variation in the published values of the critical temperature and density for methanol. Therefore, in this work, the critical parameters for methanol

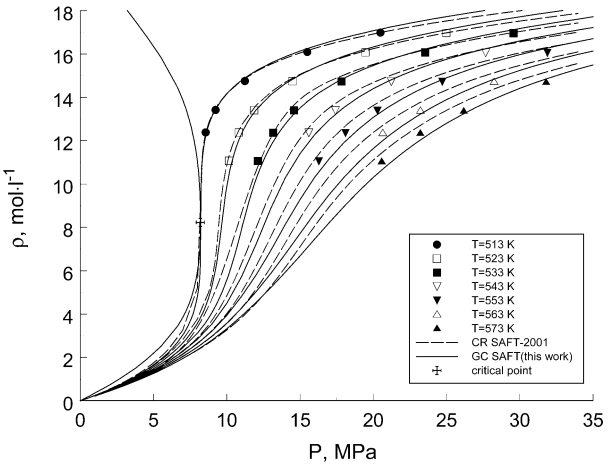

Figure 1. Experimental liquid densities for methanol[30] (symbols) as functions of pressure along the supercritical isotherms with predictions of the CR-SAFT-2001 EOS[11] (dashed curves) and the GC SAFT model (solid curves).

$$T_c = 512.75 \pm 0.03 \text{ K}, \quad \rho_c = 265 \pm 2 \text{ kg·m}^{-3} \quad (30)$$

have been found from a fit of the GC SAFT EOS to new experimental C_V data asymptotically close to the critical point obtained recently by Abdulagatov et al.[37] These values are very close to the critical temperature T_c = 512.78 K and density ρ_c = 267.8 kg·m^{-3} obtained by Bazaev et al.[31] from analysis of their *PVT* data for methanol. The critical pressure P_c = 8.196 MPa calculated with GC SAFT EOS (eq 24) is also close to the value obtained by Bazaev et al.,[31] P_c = 8.10 MPa, indicating thermodynamic self-consistency of the GC SAFT EOS applied to methanol.

The predictions of the GC SAFT model for methanol as compared with experimental data are shown in Figures 1−6. As one can see, there is very good agreement between the GCS model and the experimental data. The GC SAFT EOS reproduces the saturated pressure data at temperatures between 200 K and T_c with an average absolute deviation (AAD) of 0.64% (n = 49), the liquid density with AAD of 0.53% (n = 39), and the vapor density with AAD of 3.5% (n = 39). In the one-phase region at densities less than $2\rho_c$, the GC SAFT EOS reproduces the *PVT* data with an AAD of 1.7% (n = 262) and the liquid densities at densities greater than or equal to $2\rho_c$ with an AAD of 1.2% (n = 261). We would especially like to emphasize the excellent agreement between the predictions of the GC SAFT EOS and experimental one-phase C_P and one- and two-phase C_V data in the critical region shown in Figures 4−6. The dashed curves in Figures 4 and 5 correspond to the values calculated with the IUPAC EOS.[38] As one can see, the GC SAFT and IUPAC EOS[38] give very close predictions for the isobaric heat capacity along the near critical isobar at P = 10 MPa. However, unlike the GC SAFT EOS, the multi-parameter EOS developed by de Reuck and Craven[38] does not even qualitatively reproduce an asymptotic behavior of the isochoric heat capacity in the critical region.

In the second step, we developed the GC SAFT EOS for ethanol and higher *n*-alkanols up to heptan-1-ol. For ethanol, we adopt the same critical density as employed earlier by Kiselev and Ely[16] in the generalized corresponding states model, while for the critical temperature

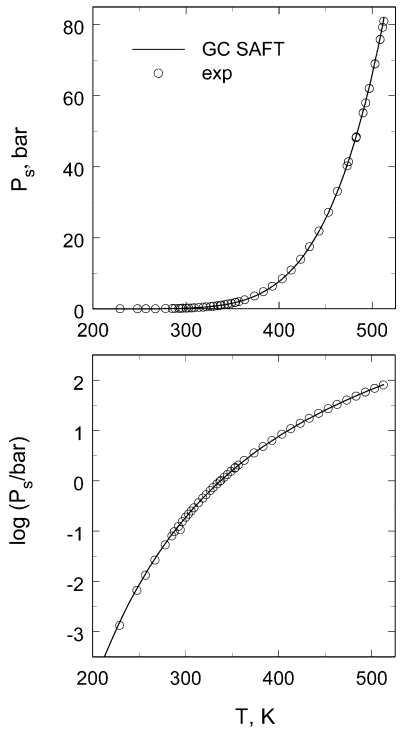

Figure 2. Saturated pressure data in normal (top) and logarithmic scale (bottom) in methanol[34,35] with predictions of the GC SAFT model (curves).

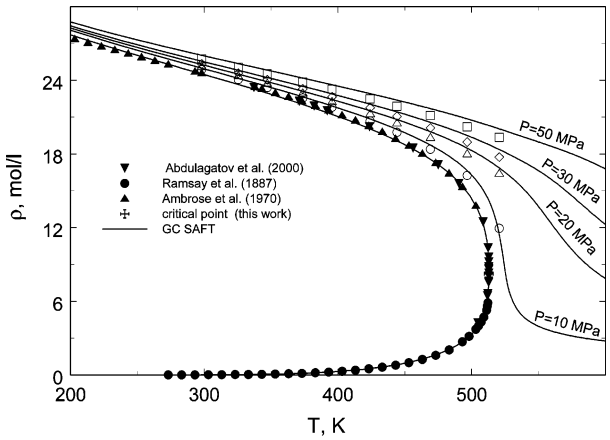

Figure 3. Experimental saturated densities for methanol[33,35,37] (filled symbols) as functions of pressure along the supercritical isotherms with predictions of the CR-SAFT-2001 EOS[11](dashed curves) and the GC SAFT model (solid curves). The empty symbols correspond to the values extracted from Bashirov's C_P measurements.[93]

we use a value obtained by Polikhronidi et al.[39] from an analysis of their new experimental C_V data in the critical region of ethanol. All other system-dependent parameters in the GC SAFT EOS for ethanol have been found from a fit of the GC SAFT EOS to VLE data[35,40,41] and one-phase *PVT* data obtained by Golubev et al.[42] and by Lo and Stiel.[43] For all other *n*-alkanols, we adopt values of the critical parameters employed earlier by Kiselev and Ely.[16] The classical SAFT parameters have been found from a fit of the GC SAFT EOS to the VLE and one-phase *PVT* data taken from refs 35, 44, and 45 for propan-ol-1; refs 35 and 45−48 for butan-1-ol; refs 49−53 for pentan-1-ol; refs 49, 50, and 53−55 for hexan-1-ol; and refs 56−58 for heptan-1-ol. The values of all system-dependent parameters of the GC SAFT EOS for *n*-alkanols are listed in Table 1. Experimental saturated

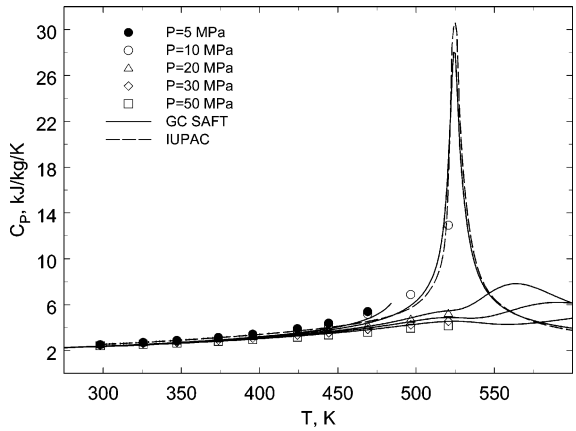

Figure 4. Isobaric heat capacity data for methanol[93] (symbols) with predictions of the IUPAC EOS[38] (dashed curve) and the GC SAFT model (solid curves).

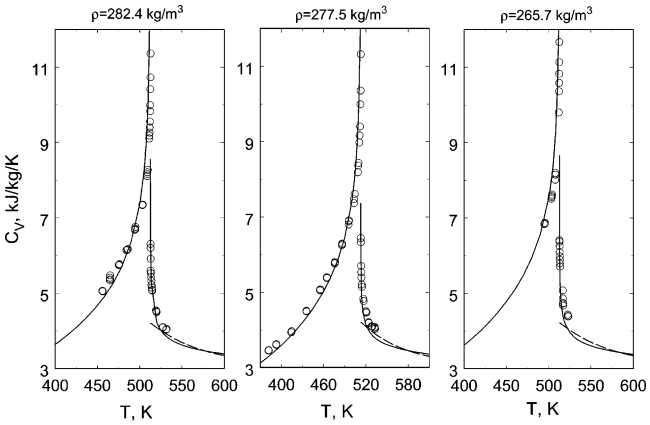

Figure 5. One- and two-phase isochoric heat capacity data along near-critical isochores for methanol[37] (symbols) with predictions of the IUPAC EOS[38] (dashed curves) and the GC SAFT model (solid curves).

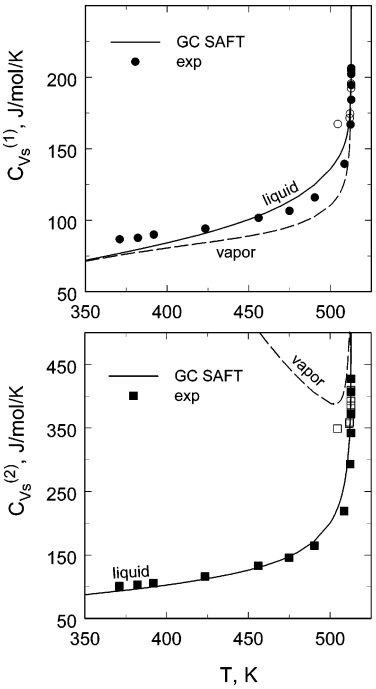

Figure 6. One- and two-phase isochoric heat capacity data along the coexistence curve for methanol[37] (symbols) with predictions of the GC SAFT model (curves).

Table 1. System-Dependent Parameters in the GC SAFT EOS for *n*-Alkanols[a]

parameter	methanol	ethanol	propanol	butanol	pentanol	hexanol	heptanol
$v^{\circ\circ}$ (mL·mol^{-1})	10.0702	9.04124	10.9362	8.48062	8.31451	10.3567	12.2227
m	2.31334	3.69051	3.93073	5.88359	6.98823	6.60700	6.04439
u^0/k_B (K)	187.884	178.583	204.010	185.350	181.097	193.770	183.051
ϵ^{AB}/k_B (K)	2563.90	2550.57	2609.13	2427.31	2196.13	2347.29	2379.45
κ^{AB}	7.5079×10^{-2}	5.0901×10^{-2}	1.9266×10^{-2}	3.5428×10^{-2}	7.9569×10^{-2}	6.1344×10^{-2}	3.2477×10^{-1}
M_w	32.042	46.069	60.097	74.123	88.150	102.177	116.204
T_c (K)	512.75	514.45	536.71	562.90	588.15	611.40	633.15
ρ_c (mol·L^{-1})	8.2700	5.9880	4.5830	3.6500	3.030	2.6250	2.3120
P_c (MPa)[a]	8.1959	6.1912	5.1715	4.41703	3.8562	3.3823	3.1137

[a] Calculated with the GC SAFT EOS.

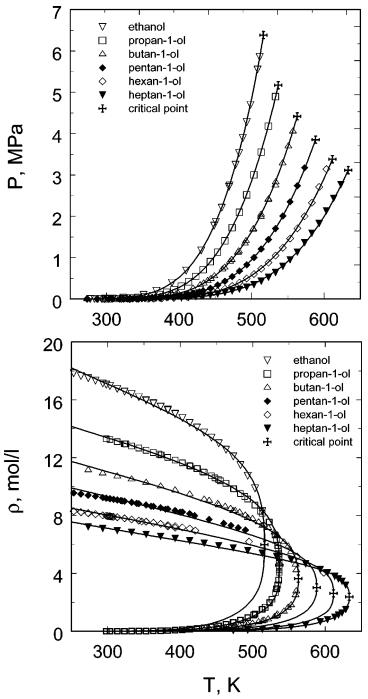

Figure 7. Saturated pressure (top) and saturated density (bottom) data for ethanol,[35,40,41] propan-ol-1,[35,44] butan-1-ol,[35,46−48] pentan-1-ol,[49−51,53] hexan-1-ol,[49,50,53,54] and heptan-1-ol[58] (symbols) with predictions of the GC SAFT model (curves).

pressure and liquid and vapor density data in comparison with values calculated with the crossover GC SAFT EOS are shown in Figure 7. For all fluids shown in Figure 7, the GC SAFT EOS reproduces the saturated pressure and liquid density data with an AAD of less than 1% and the vapor densities with an AAD of about 3−4%. Figures 8 and 9 compare the predictions of the GC SAFT EOS with experimental one-phase *PVT* (Figure 8) and one- and two-phase C_V (Figure 9) data for ethanol. Again, excellent agreement between the predictions of the GC SAFT EOS and experimental data for both *PVT* and C_V data sets is observed. The dashed lines in Figure 9 correspond to the values of the isochoric heat capacity calculated with a new fundamental equation for ethanol developed by Dillon and Penoncello.[59] As one can see, this EOS, similar to the IUPAC EOS for methanol considered above (see Figure 5), fails to reproduce the C_V data in the critical region, while the GC SAFT EOS even asymptotically close to the critical point, at $T \rightarrow \pm T_c$, is in excellent agreement with experimental data.

4. Surface Tension

As we mentioned above, GC SAFT EOS based on the sine model can be extended into the metastable region;

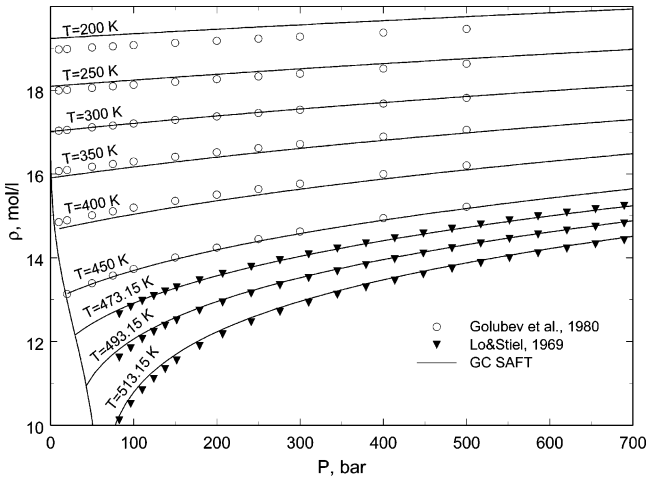

Figure 8. Experimental liquid densities for ethanol[42,43] (symbols) as functions of pressure along sub- and supercritical isotherms with predictions of the CR GC SAFT model (solid curves).

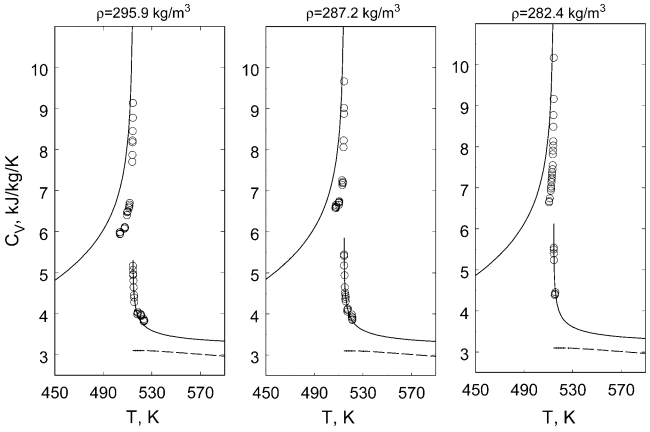

Figure 9. One- and two-phase isochoric heat capacity data along near-critical isochores for ethanol[39] (symbols) with predictions of the fundamental EOS[59] (dashed curves) and the GC SAFT model (solid curves).

at subcritical temperatures, it represents analytically connected van der Waals loops. This, together with the high accuracy of the representation of the *PVT* and VLE surface near to and far from the critical point, allows us to use the GC SAFT EOS in the generalized crossover density functional theory (DFT) model for the surface tension of associating fluids. The GC DFT expression for the surface tension of pure fluids is given by[16]

$$\sigma(T) = c_0^{1/2} \int_{\rho_V}^{\rho_L} \sqrt{\Delta \hat{A}(T, \rho)} \mathrm{d}\rho \qquad (31)$$

where $\rho_{V,L}$ corresponds to the saturated vapor (V) and liquid (L) densities at a given temperature T; $\Delta\hat{A}(T, \rho) = A(T, \rho) - \rho\mu(T, \rho_{V,L})$ is an excess part of the Helmholtz

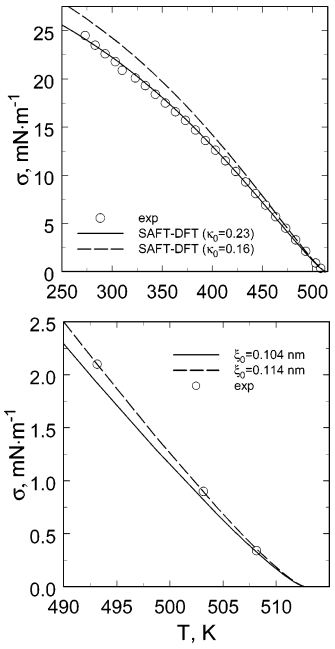

Figure 10. Surface tension data for methanol[46] (symbols) with predictions of the GC SAFT-DFT model with $\kappa_0 = 0.23$ (solid curves) and $\kappa_0 = 0.16$ (dashed curves).

free energy density in the two-phase region at $\rho_V \leq \rho \leq \rho_L$; and $\mu(T, \rho_{V,L}) = (\partial\rho A/\partial\rho)_T$ is the chemical potential of the bulk fluid along the saturation curve $\rho = \rho_{V,L}(T)$. In eq 31, the Helmholtz free energy $A(T, \rho) = a(T, v)RT$ is calculated with the GC expression for $a(T, v)$ (eq 20) and the parameter c_0, which is directly related to the asymptotic critical amplitude of the correlation length:[60]

$$\xi_0^+ = (c_0\Gamma_0^+)^{1/2} \tag{32}$$

(Γ_0^+ is an amplitude in the asymptotic power law $\chi_T(\rho_c, \tau) = \Gamma_0^+\tau^{-\gamma}$ for the reduced isothermal compressibility $\chi_T = \rho T(\partial\rho/\partial P)_T P_c\rho_c^{-2}\, T_c^{-1}$) can be estimated for associating fluids with the expression[16]

$$c_0 = (1 - \kappa_0)^2 k_B T \rho_c^{1/3} \tag{33}$$

where the system-dependent coefficient $\kappa_0 < 1$ can be extracted from the surface tension measured at $T = 0.7T_c$, or nearby values.

In this work, we applied the GC SAFT-DFT model for the calculation of the surface tension in methanol, ethanol, and butan-1-ol. Comparisons of the predicted values of the surface tension with experimental data are shown in Figures 10 and 11. As one can see from Figure 10, in a wide temperature range, at $0.5T < T < T_c$, a better result for the surface tension in methanol can be achieved with the parameter $\kappa_0 = 0.23$ (or $\xi_0 = 0.104$ nm). However, in the asymptotic critical region at $|\tau| \leq 0.02$, the GC SAFT-DFT model reproduces the surface tension data better with the parameter $\kappa_0 = 0.16$ or $\xi_0 = 0.114$ nm. For ethanol and butan-1-ol, good agreement with experimental data is achieved with the parameter $\kappa_0 = 0.16$, or the same with the critical amplitudes $\xi_0 = 0.111$ nm for ethanol and $\xi_0 = 0.124$ nm butan-1-ol, respectively (see Figure 11).

5. Thermal Conductivity

For the thermal conductivity of the *n*-alkanols, we use a crossover decoupled-mode theory (DMT) model for the

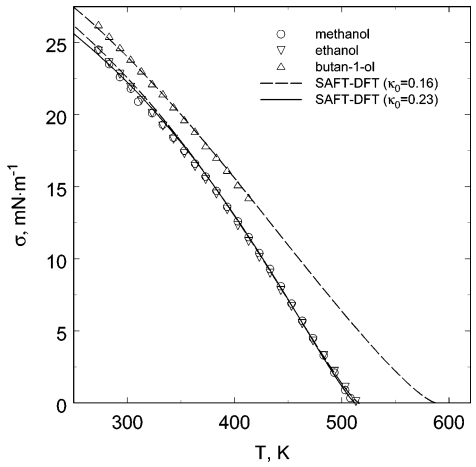

Figure 11. Surface tension data for methanol, ethanol, and butan-1-ol[46] (symbols) with predictions of the GC SAFT-DFT (curves).

transport coefficients of pure fluids and fluid mixtures developed by Kiselev and Kulikov.[61,62] In the limit of pure components, the crossover expression for the thermal conductivity takes the form[61−63]

$$\lambda = \frac{k_B T \rho C_P}{6\pi\eta_b \hat{\xi}}\Omega(z) + \lambda_b \tag{34}$$

where η_b is the viscosity, and λ_b is a background part of the thermal conductivity that can be represented as a sum of the dilute-gas and the residual contributions

$$\lambda_b(\rho, T) = \lambda^\circ(T) + \Delta\lambda_r(\rho, T) \tag{35}$$

where λ° is the dilute-gas thermal conductivity, which depends only on temperature, and $\Delta\lambda_r$ is the residual thermal conductivity. The crossover function $\Omega(z) = \Omega(q_D\hat{\xi})$ in eq 34 is given by

$$\Omega(z) = \frac{2}{\pi}\left[\tan^{-1}(z) - \frac{1}{\sqrt{1 + y_{1D}z}}\tan^{-1}\left(\frac{z}{\sqrt{1 + y_{1D}z}}\right)\right] \tag{36}$$

where

$$y_{1D} = \frac{6\pi\eta_b^2}{k_B T \rho q_D(\phi_1 + y_1^{-1})}, \quad y_1 = \frac{k_B T \rho C_P}{6\pi\eta_b\hat{\xi}\lambda_b} \tag{37}$$

In eqs 34−37, q_D is a cutoff wavenumber, the renormalized correlation length is given by[63]

$$\hat{\xi} = \xi_{OZ}\exp\left(-\frac{1}{q_D\xi_{OZ}}\right) \tag{38}$$

where $\xi_{OZ} = \xi_0\sqrt{\chi_T/\Gamma_0}$ corresponds to the Ornstein−Zernike approximation for the correlation length[60], and $\phi_1 = \phi(k_{1D}\hat{\xi}) = \phi(z)$ is the dynamical scaling function[61,62]

$$\phi(z) = \frac{3[1 + z^2 + (z^3 - z^{-1})\tan^{-1}(z)]}{4z^2(1 + z^2)} \tag{39}$$

calculated at a constant value of the wavenumber $k_{1D} = 0.1q_D$. Asymptotically close to the critical point at $q_D\hat{\xi} \gg 1$, the parameter $y_1 \gg 1$, the crossover function $\Omega(z)$ approaches unity, and the thermal conductivity along

Table 2. Parameters for the Second Viscosity Virial Coefficient,[65] Equation 44

i	b_i	t_i	i	b_i	t_i
0	−19.572 881	0	5	2491.659 7	−1.25
1	219.739 99	−0.25	6	−787.260 86	−1.50
2	−1015.322 6	−0.50	7	14.085 455	−2.50
3	2471.012 5	−0.75	8	−0.346 641 58	−5.50
4	−3375.171 7	−1.00			

the critical isochore diverges at $\tau \rightarrow +0$ as $\lambda \propto \tau^{-\gamma/2}$. Far from the critical point, at $q_D\hat{\xi} \ll 1$, the crossover function $\Omega(z) \rightarrow 0$, and the thermal conductivity λ becomes equal to its background part λ_b.

In this work, we applied the GC SAFT-DMT model for the calculation of the thermal conductivity of methanol and ethanol in a wide range of temperatures and pressures, including the critical and supercritical regions. All thermodynamic properties in the GC SAFT-DMT model (eqs 36−39) are calculated with the GC SAFT EOS, with the cutoff wavenumber $q_D^{-1} = 3\xi_0$, where for the critical amplitude ξ_0 we adopt the values obtained in the GC SAFT-DFT model for the surface tension

$$\xi_0^{C_1OH} = 0.114 \text{ nm}, \quad \xi_0^{C_2OH} = 0.111 \text{ nm}, \quad \xi_0^{C_4OH} = 0.124 \text{ nm} \quad (40)$$

The shear viscosity (η_b) in eqs 34 and 37 is an analytic function of the temperature and density. For methanol, we adopted the expression given by Xiang et al.[64] that represents the data in the liquid and vapor phase up to pressures of about 500 MPa to about 3%. For the viscosity of ethanol, we are not aware of any wide-ranging, accurate correlations, so we present one here. In this work, η_b has been represented as the sum of a dilute-gas contribution and a residual term[65]

$$\eta_b(\rho, T) = \eta^\circ(T)[1 + B_\eta(T)\rho] + \Delta_H\eta(\rho, T) \quad (41)$$

The term $\eta^\circ(T)$ represents the viscosity in the limit of zero density, $B_\eta(T)$ is the second virial coefficient for viscosity based on the Rainwater−Friend theory,[66] and $\Delta_H\eta(\rho, T)$ is the contribution that represents the higher-order density terms as a function of the absolute temperature T and density ρ.

We approximated the viscosity η° of ethanol in the zero-density limit using a polynomial in temperature[67]

$$\eta^\circ(T) = -1.03116 + 3.48379 \times 10^{-2}\, T - 6.50264 \times 10^{-6}\, T^2 \quad (42)$$

where T is in K and the viscosity is in μPa·s. The Rainwater−Friend term[66,68] is found using

$$B_\eta(T) = N_A\sigma^3 B_\eta^*(T^*) \quad (43)$$

where N_A is the Avogadro constant, and we used the correlation for B_η^* given by Vogel et al.[65]

$$B_\eta^*(T^*) = \sum_{i=0}^{8} b_i (T^*)^{t_i} \quad (44)$$

with parameters b_i and the exponents t_i taken from Vogel et al.[65] that are given in Table 2. For the Lennard−Jones parameters we adopted the values $\sigma =$ 0.453 nm and $\epsilon/k = 362.6$ K given in Reid et al.[69]

Table 3. Parameters for the Viscosity Correlation, Equations 45 and 46

coefficient		coefficient	
α_{20}	0.131194057	α_{32}	−0.110578307
α_{21}	−0.382240694	c_1	23.7222995
α_{22}	0	c_2	−3.38264465
α_{30}	−0.0805700894	c_3	12.7568864
α_{31}	0.153811778		

We expressed the higher density terms $\Delta_H\eta(\rho, T)$ in terms of the reduced density $\delta = \rho/\rho_R$ and the reduced temperature $\tau = T/T_R$ using the form[70]

$$\Delta_H\eta(\rho,T) = 1000\left(\sum_{j=2}^{3}\sum_{k=0}^{2}\alpha_{jk}\frac{\delta^j}{\tau^k} + c_1\delta\left(\frac{1}{\delta_0 - \delta} - \frac{1}{\delta_0}\right)\right) \quad (45)$$

$$\delta_0 = c_2 + c_3\sqrt{\tau} \quad (46)$$

where the viscosity is in μPa·s and the reducing parameters were $T_R = 513.9$ K and $\rho_R = 5.991$ mol/L.

We used primarily the data of Golubev and Petrov[71] as given in Golubev[72] and several additional, smaller data sets[73−78] that cover a wide range of temperature and pressure conditions that included pressures up to 100 MPa and temperatures from 273 to 538 K, and regressed the data with the statistical package ODRPACK[79] in order to obtain the coefficients given in Table 3. The densities of ethanol used in the regression were obtained from the equation of state of Dillon and Penoncello.[59] The correlation represents the Golubev and Petrov[71,72] data set with and average absolute deviation of 1.86%, the Assael and Polimatidou[73] data to 0.7%, Papaioannou and Panayiotou[76] data to 2.1%, Papanastasiou and Ziogas[77] data to 0.4%, Lee et al.[75] data to 1.0%, Bingham et al.[74] data to 1.6%, and Phillips and Murphy[78] data to 1.1%.

We approximated the dilute-gas contribution for the thermal conductivity of methanol by adopting the correlation[80]

$$\lambda^{(0)}(T) = 5.7992 \times 10^{-7}\, T^{1.7862} \quad (47)$$

while for ethanol we used the equation recommended by the DIPPR DIADEM program[80]

$$\lambda^\circ(T) = \frac{-10.109 \times 10^{-3}\, T^{0.6475}}{1.0 - 7332/T - 268000/T^2} \quad (48)$$

where the temperature unit is K and the thermal conductivity units are W·m^{-1}·K^{-1}. For the residual contribution in both fluids, methanol and ethanol, we use here a polynomial in temperature and density

$$\Delta\lambda_r(\rho, T) = \sum_{i=1}^{3}\left(b_{i,1} + b_{i,2}\frac{T}{T_c}\right)\left(\frac{\rho}{\rho_c}\right)^i \quad (49)$$

which has recently been shown to accurately represent hydrocarbon fluids such as isobutane,[81] butane,[82] and propane.[83] The parameters $b_{i,j}$ ($i = 1-3$, $j = 1, 2$) in the residual contribution have been found from a fit of the GC SAFT-DMT model to the selected data sets for methanol[46,84−90] and ethanol[46,91,92] that cover a wide range of temperature and pressure conditions above and below the critical point. The values of the coefficients $b_{i,j}$ in eq 49 for methanol and ethanol are listed in Table 4, and comparisons with the experimental thermal

Table 4. Coefficients $b_{i,j}$ in Equation 48 for Thermal Conductivity of Methanol and Ethanol

parameter	methanol	ethanol
$b_{1,1}$	3.11820803E−01	1.06917458E−01
$b_{2,1}$	−2.07326311E−01	−8.65012441E−02
$b_{3,1}$	4.09897792E−02	2.12220237E−02
$b_{1,2}$	−2.18459475E−01	−5.95897870E−02
$b_{2,2}$	1.71891658E−01	6.14073818E−02
$b_{3,2}$	−3.20792858E−02	−1.00317135E−02

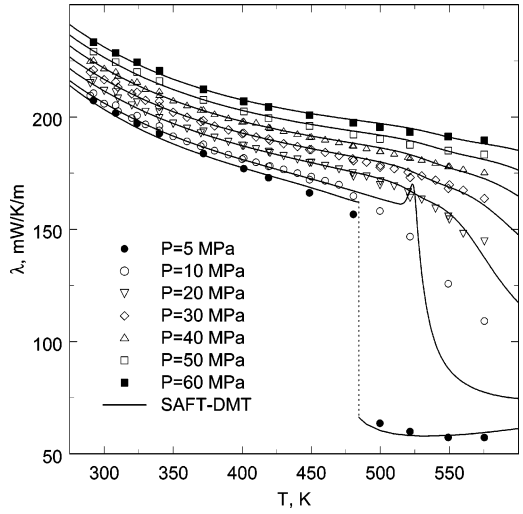

Figure 12. Thermal conductivity data for methanol[28,84] (symbols) with predictions of the GC SAFT-DMT model (curves).

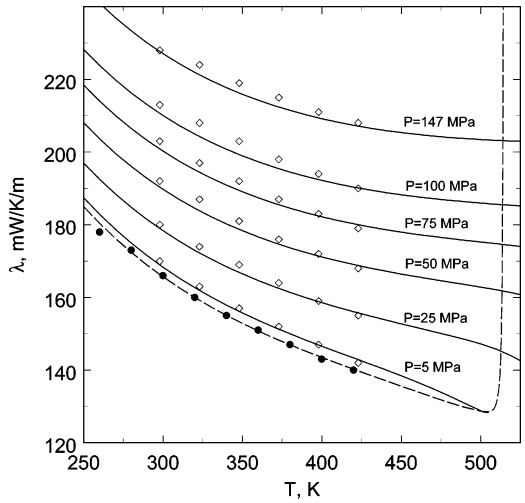

Figure 13. Thermal conductivity data for ethanol along isobars[91] (empty symbols) and along the saturated curve[94] (filled symbols) as a function of temperature with predictions of the GC SAFT-DMT model (curves).

conductivity data are shown in Figures 12−14. For both substances, very good agreement between the GC SAFT-DMT model and experimental thermal conductivity data is observed. The GC SAFT-DMT model reproduces all thermal conductivity data for methanol (n = 430) and ethanol (n = 230) with an AAD of 0.85%. The sharp maxima of the thermal conductivity observed at P = 10 MPa and T = 512 K in methanol (see Figure 12) and at near critical pressures at T = 520 K for ethanol (see Figure 14) correspond to the critical enhancements caused by long-range density fluctuations as described by the first term in right-hand side of eq 34. In Figure 15 we show the thermal conductivity for methanol as a function of density calculated along the selected isobars and isotherms with the GC SAFT-DMT model. As one

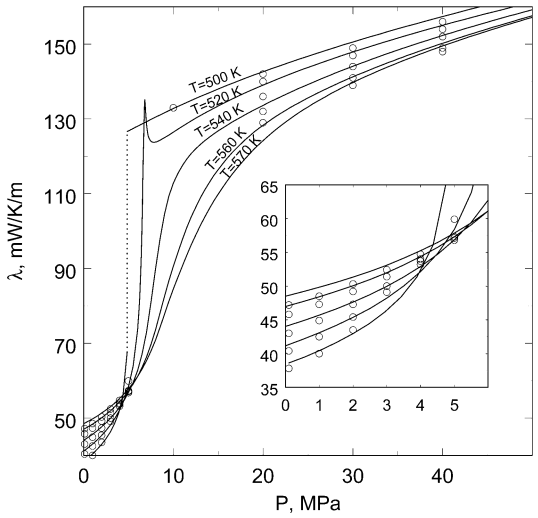

Figure 14. Thermal conductivity data for ethanol along isotherms[94] (symbols) as a function of pressure with predictions of the GC SAFT-DMT model (curves).

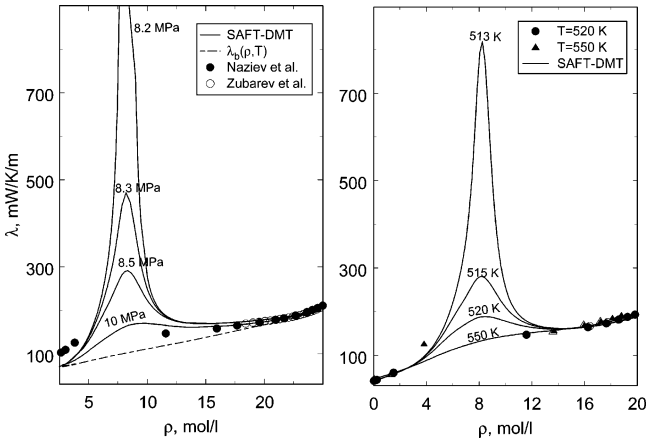

Figure 15. Thermal conductivity data for methanol[28,84] (symbols) along isobars (left) and along isotherms (right) as a function of density with predictions of the GC SAFT-DMT model (curves).

can see, the maxima of the thermal conductivity, observed at $\rho \cong \rho_c$, increase drastically as the pressure and temperature approach their critical values.

The thermal diffusivity ($D_T = \lambda/\rho C_P$) is another property that exhibits a strong anomalous behavior in the critical region. Since the thermal diffusivity requires a simultaneous calculation of the thermal conductivity, isobaric heat capacity, and density, it is a good test for the physical self-consistency of the model. In Figure 16 we show comparisons between GC SAFT-DMT predictions and thermal diffusivity data in methanol obtained by Bushirov.[93] Agreement between the GC SAFT-DMT calculations and experimental data is fairly good. Since no experimental D_T data have been used for the optimization of the GC SAFT-DMT model, we consider this result as additional evidence of the physical self-consistency of the GC SAFT DMT model.

6. Conclusions

The molecularly based SAFT EOS has proven to be very versatile for the prediction of phase equilibria in associating fluids. However, in common with all analytic EOS, the SAFT EOS exhibits classical behavior in the critical region rather than the nonanalytical, singular behavior caused by the density fluctuations, which

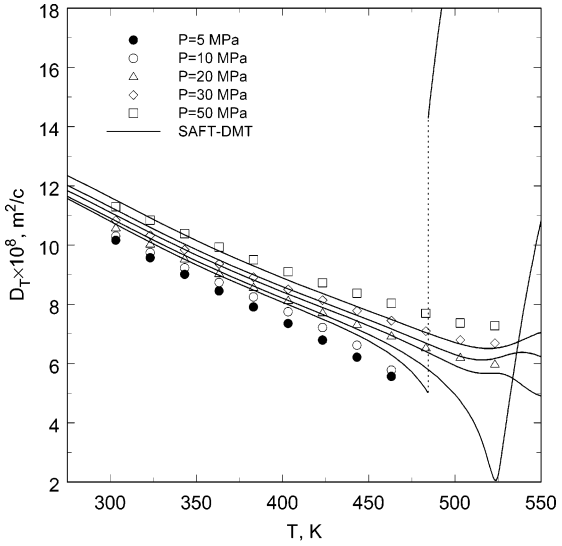

Figure 16. Thermal diffusivity data for methanol along the isobars[93] (symbols) as a function of temperature with predictions of the GC SAFT-DMT model (curves).

anomalously increase in the vicinity of the critical point of pure fluids. As a result, accurate agreement over the whole phase diagram cannot be obtained with analytic SAFT equations and they must be localized to either the critical or subcritical regions. The first step in developing a crossover SAFT equation, which incorporates the scaling laws in the critical region and is transformed into the original analytical−classical EOS far from the critical point, was made by Kiselev and Ely.[10] Later, several different types of crossover SAFT EOS were developed.[11−15] It has been shown that crossover SAFT equations are able to accurately describe the whole fluid phase diagram representing not only the VLE, but also the *PVT* properties in long-chain, polar, and associating fluids. However, except for the CR SAFT EOS for propan-1-ol,[18] no attempt was made to develop a GC SAFT EOS for the VLE, *PVT*, C_P, and C_V properties, and until now no generalized crossover SAFT model for the thermodynamic, interfacial, and transport properties in associating fluids has been developed.

In this work, we have developed a GC SAFT EOS model for *n*-alkanols by incorporating the crossover approach developed by Kiselev into the analytical SAFT equation for associating fluids developed by Huang and Radoz,[4−6] model 2B.[4] With only four adjustable parameters, the GC SAFT EOS describes the VLE, *PVT*, C_P, and C_V properties of *n*-alkanols with an accuracy comparable, and for the near critical C_V data even higher, than that achieved with empirical multiparameter equations of state. The GC SAFT EOS not only gives excellent representation of the thermodynamic properties in the one-phase region but is also capable of reproducing the van der Waals loops in the two-phase region. The molecularly based, rather than empirical, nature of the GC SAFT EOS allowed us to incorporate the GC SAFT EOS into the generalized crossover DFT integrals,[16] and thus develop a GC SAFT-DFT model for the surface tension of associating fluids. By incorporating the GC SAFT EOS into the crossover DMT equations obtained by Kiselev and Kulikov,[61,62] we have also developed a GC SAFT-DMT model for the transport properties. The GC SAFT-DFT/DMT model has been tested against experimental surface tension, thermal conductivity, and thermal diffusivity data for methanol, ethanol, and butan-1-ol. In addition to the classical SAFT parameters, the GC SAFT-DFT/DMT model requires the asymptotic critical amplitude of the correlation length and the background contributions for the transport coefficients as input, and has proven to be very accurate. Except for the generalized crossover model for simple fluids developed recently by Kiselev and Ely,[17] we are not aware of any other molecular or empirical models describing the thermodynamic, interfacial, and transport properties in pure fluids with comparable accuracy and physical self-consistency. The next step is applying this model to mixture calculations. Work in this direction is now in progress, and the results will be reported in future publications.

Acknowledgment

Research at the Colorado School of Mines was supported by the U.S. Department of Energy, Office of Basic Energy Sciences, under Grant DE-FG03-95ER14568. I.M.A. thanks the Physical and Chemical Properties Division at the National Institute of Standards and Technology for the opportunity to work as a Guest Researcher at NIST during the course of this research.

Literature Cited

(1) Jackson, G.; Chapman, W. G.; Gubbins, K. E. Phase equilibria of associating fluids. Spherical molecules with multiple bonding sites. *Mol. Phys.* **1988**, *65*, 1−31.

(2) Chapman, W. G.; Gubbins, K. E.; Jackson, G.; Radosz, M. SAFT equation-of-state solution model for associating fluids. *Fluid Phase Equilib.* **1989**, *52*, 31−38.

(3) Chapman, W. G.; Gubbins, K. E.; Jackson, G.; Radosz, M. New reference equation of state for associating fluids. *Ind. Eng. Chem. Res.* **1990**, *29*, 1709−1721.

(4) Huang, S. H.; Radosz, M. Equation of state for small, large, polydisperse, and associating molecules. *Ind. Eng. Chem. Res.* **1990**, *29*, 2284−2294.

(5) Huang, S. H.; Radosz, M. Phase behavior of reservoir fluids. V: SAFT model of carbon dioxide and bitumen systems. *Fluid Phase Equilib.* **1991**, *70*, 33−54.

(6) Huang, S. H.; Radosz, M. Equation of state for small, large, polydisperse, and associating molecules: extension to fluid mixtures. *Ind. Eng. Chem. Res.* **1991**, *30*, 1994−2005.

(7) Fu, Y.-H.; Sandler, S. I. A Simplified SAFT equation of state for associating compounds and mixtures. *Ind. Eng. Chem. Res.* **1995**, *34*, 1897−1996.

(8) Kraska, T.; Gubbins, K. E. Phase equilibria calculations with a modified SAFT equation of state. 1. Pure alkanes, alkanols, and water. *Ind. Eng. Chem. Res.* **1996**, *35*, 4727−4737.

(9) Kiselev, S. B. Cubic crossover equation of state. *Fluid Phase Equilib.* **1998**, *147*, 7−23.

(10) Kiselev, S. B.; Ely, J. F. Crossover SAFT equation of state: application for normal alkanes. *Ind. Eng. Chem. Res*. **1999**, *38*, 4993−5004.

(11) Kiselev, S. B.; Ely, J. F.; Adidharma, H.; Radosz, M. A crossover equation of state for associating fluids. *Fluid. Phase. Equilib.* **2001**, *183−184*, 53−64.

(12) Hu, Z.-Q.; Yang, J.-C.; Li, Y.-G. Crossover SAFT equation of state for pure supercritical fluids. *Fluid Phase Equilib*. **2003**, *205*, 1−15.

(13) Hu, Z.-Q.; Yang, J.-C.; Li, Y.-G. Crossover SAFT-BACK equation of state for pure CO_2 and H_2O. *Fluid Phase Equilib*. **2003**, *205*, 25−36.

(14) McCabe, C.; Kiselev, S. B. A crossover SAFT-VR equation of state for pure fluids: preliminary results for light hydrocarbons. *Fluid Phase Equilib.* **2004**, *219*, 3.

(15) McCabe, C.; Kiselev, S. B. Application of crossover theory to the SAFT-VR equation of state: SAFT-VRX for pure fluids. *Ind. Eng. Chem. Res.* **2004**, *43*, 2839.

(16) Kiselev, S. B.; Ely, J. F. Generalized corresponding states model for bulk and interfacial properties of pure fluids and fluid mixtures. *J. Chem. Phys.* **2003**, *119*, 8645−8662.

(17) Kiselev, S. B.; Ely, J. F. Generalized crossover description of the thermodynamic and transport properties in pure fluids. *Fluid Phase Equilib.* **2004**, *222/223*, 149−159.

(18) Kiselev, S. B.; Ely, J. F.; Abdulagatov, I. M.; Magee, J. W. Crossover SAFT equation of state and thermodynamic properties of propan-1-ol. *Int. J. Thermophys.* **2000**, *6*, 1373−1405.

(19) Carnahan, N. F.; Starling, K. E. Equation of state for nonattracting rigid spheres. *J. Chem. Phys.* **1969**, *51*, 635−636.

(20) Chen, S. S.; Kreglewski, A. Applications of the augmented van der Waals theory of fluids. I. Pure fluids. *Ber. Bunsen-Ges. Phys. Chem.* **1977**, *81*, 1048−1051.

(21) Anisimov, M. A.; Kiselev, S. B. Universal crossover approach to description of thermodynamic properties of fluids and fluid mixtures. In *Sov. Technol. Rev. B. Therm. Phys., Part 2* **1992**, *3*, 1−121.

(22) Sengers, J. V.; Levelt Sengers, J. M. H. Thermodynamic behavior of fluids near the critical point. *Annu. Rev. Phys. Chem.* **1986**, *37*, 189−222.

(23) Kiselev, S. B.; Ely, J. F. Simplified crossover SAFT equation of state. *Fluid Phase Equilib.* **2000**, *174*, 93−119.

(24) Wegner, F. J. Corrections to scaling laws. *Phys. Rev. B* **1972**, *5*, 4529−4536.

(25) Kiselev, S. B.; Sengers, J. V. An improved parametric crossover model for the thermodynamic properties of fluids in the critical region. *Int. J. Thermophys.* **1993**, *14*, 1−32.

(26) Kiselev, S. B.; Rainwater, J. C.; Huber, M. L. Binary mixtures in and beyond the critical region: thermodynamic properties. *Fluid Phase Equilib.* **1998**, *150/151*, 469−478.

(27) Belyakov, M. Y.; Kiselev, S. B. Crossover-behavior of the susceptibility and the specific heat near a 2nd-order phase-transition. *Physica A* **1992**, *190*, 75−94.

(28) Zubarev, V. N.; Prusakov, P. G.; Sergeev, L. V. *Thermophysical Properties of Methyl Alcohol*; GSSSD: Moscow, 1973.

(29) Finkelstein, R. S.; Stiel, L. I. The PVT behavior of methanol at elevated pressures and temperatures. *Chem. Eng. Prog. Symp. Ser.* **1970**, *16* (98), 11−15.

(30) Straty, G. C.; Palavra, A. M. F.; Bruno, T. J. PVT properties of methanol at temperatures to 300 degrees C. *Int. J. Thermophys.* **1986**, *7*, 1077−1089.

(31) Bazaev, A. R.; Abdulagatov, I. M.; Magee, J. W.; Bazaev, E. A. *Int. J. Thermophys.* (to be submitted for publication).

(32) Machado, R. S.; Streett, W. B. Equation of state and thermodynamic properties of liquid methanol from 298 to 489 K. *J. Chem. Eng. Data* **1983**, *28*, 218−223.

(33) Ramsay, W.; Young, S. On evaporation and dissociation. Part V. A study of the thermal properties of methyl-alcohol. *Philos. Trans. R. Soc. London A* **1887**, *178*, 313−334.

(34) Donham, W. E. VLE data for 1-methanol. PhD, The Ohio State University, Columbus, OH, 1953.

(35) Ambrose, D.; Sprake, C. H. Thermodynamic properties of organic oxygen compounds. XXV. Vapor pressures and normal boiling temperatures of aliphatic alcohols. *J. Chem. Thermodyn.* **1970**, *2*, 631−645.

(36) Abdulagatov, I. M.; Dvorynchikov, V. I.; Aliev, M. M.; Kamalov, A. N. Isochoric heat capacity of 0.5 water and 0.5 methanol mixtures at subcritical and supercritical conditions. In *Steam, Water, and Hydrothermal Systems*: *Proceedings of the 13th International Conference on the Properties of Water and Steam*; Tremaine, P. R., Irish, D. E., Balakrishnan, P. V., Eds.; NRC Research Press: Toronto, 2000; pp 157−164.

(37) Abdulagatov, I. M.; Polikhronidi, N. G.; Abdulrashidova, A.; Magee, J. W.; Kiselev, S. B.; Ely, J. F. Thermodynamic properties of methanol in the near-critical and supercritical region. *Int. J. Thermophys.* (submitted for publication).

(38) de Reuck, K. M.; Craven, R. J. B. *Methanol. International Thermodynamic Tables of the Fluid State-12*; Blackwell: Oxford, 1993.

(39) Polikhronidi, N. G.; Abdulagatov, I. M.; Stepanov, G. V.; Magee, J. W. Isochoric heat capacity of ethanol in the near-critical and supercritical region. (manuscript in preparation).

(40) Mischenko, K. P.; Subbotina, V. V. Vapor pressure of ethyl alcohol at temperatures from 4 to 460. *J. Appl. Chem. USSR* **1967**, *40*.

(41) Gallaugher, A. F.; Hibbert, H. Studies on reactions relating to carbohydrates and polysaccharides. LIV. The surface tension constants of the polyethylene glycols and their derivatives. *J. Am. Chem. Soc.* **1937**, *59*, 2514.

(42) Golubev, I. F.; Vasil'kovskaya, T. N.; Zolin, V. S. *Inzh.-Fiz. Zh. (Russ.)* **1980**, *45*, 668−670.

(43) Lo, H. Y.; Stiel, L. I. The PVT behavior of ethyl alcohol at elevated pressures and temperatures. *Ind. Eng. Chem. Fundam.* **1969**, *39*, 713−718.

(44) Kubicek, A. J.; Eubank, P. T. Thermodynamic properties of *n*-propanol. *J. Chem. Eng. Data* **1972**, *17*, 232−235.

(45) Golubev, I. F.; Vasil'kovskaya, T. N.; Zolin, B. C. Density of *n*-propanol and iso-propanol at different temperatures and pressures. *Proc. GIAP (Russ.)* **1979**, *54*, 5−15.

(46) Vargaftik, N. B. *Handbook of Physical Properties of Liquids and Gases*, 2nd ed.; Hemisphere Publishing Co.: New York, 1983.

(47) Efremov, Y. V. *Russ. J. Phys. Chem.* **1966**, *40*, 1240.

(48) Ambrose, D.; Townsend, R. Thermodynamic properties of organic oxygen compounds. Part IX. The critical properties and vapour pressures, above five atmospheres, of six aliphatic alcohols. *J. Chem. Soc.* **1963**, 3614−3625.

(49) Stull, D. R. Vapor pressure of pure substances. *Ind. Eng. Chem.* **1947**, *39*, 517−540.

(50) Wilhoit, R. C.; Zwolinski, B. J. Physical and thermodynamic properties of aliphatic alcohols. *J. Phys. Chem. Ref. Data* **1973**, *2*, 1−407.

(51) Hales, J. L.; Ellender, J. H. Liquid densities from 293 to 434 K of nine aliphatic alcohols. *J. Chem. Thermodyn.* **1976**, *8*, 1177−1184.

(52) Zolin, V. S.; Golubev, I. F.; Vasil'kovskaya, T. N. *Tr. GIAP (Russ.)* **1979**, *54*, 22−25.

(53) Hall, K. R. *Selected Values of Properties of Chemical Compounds*; Thermodynamics Research Center, Texas A&M University: College Station, TX, 1980.

(54) Ortega, J. Densities and thermal expansivities of hexanol isomers at moderate temperatures. *J. Chem. Eng. Data* **1985**, *30*, 5−7.

(55) Gylmanov, A. A.; Apaev, T. A.; Akhmedov, L. A.; Lipovetskii, S. I. *Izv. Vyssh. Ucheb. Zaved., Neft Gaz*. **1979**, *22*, 55−56.

(56) Golubev, I. F.; Vasil'kovskaya, T. N.; Zolin, V. S.; Shelkovenko, A. E. *Inzh.-Fiz. Zh. (Russ.)* **1981**, *45*, 313−318.

(57) Garg, S. K.; Banipal, T. S.; Ahluwalia, J. C. *J. Chem. Eng. Data* **1993**, *57*, 227−230.

(58) Hall, K. R. *TRC Thermodynamic Tables—Nonhydrocarbons*; Thermodynamics Research Center, Texas A&M University: College Station, TX, 1987.

(59) Dillon, H. E.; Penoncello, S. G. A fundamental equation for calculation of the thermodynamic properties of ethanol. *Int. J. Thermophys.* **2004**, *25*, 321−335.

(60) Landau, L. D.; Lifshitz, E. M. *Statistical Physics, Part 1*; Pergamon Press: New York, 1980; Vol. 5.

(61) Kiselev, S. B.; Kulikov, V. D. Thermodynamic and transport properties of fluids and fluid mixtures in the extended critical region. *Int. J. Thermophys.* **1997**, *18*, 1143−1179.

(62) Kiselev, S. B.; Kulikov, V. D. Crossover behavior of the transport coefficients of critical binary mixtures. *Int. J. Thermophys.* **1994**, *15*, 283−308.

(63) Kiselev, S. B.; Huber, M. L. Transport properties of carbon dioxide + ethane and methane + ethane mixtures in the extended critical region. *Fluid Phase Equilib.* **1998**, *142*, 253−280.

(64) Xiang, H. W.; Huber, M. L.; Laesecke, A. A new reference correlation for the viscosity of methanol applicable over the entire fluid surface. *J. Phys. Chem. Ref. Data* (submitted for publication).

(65) Vogel, E.; Küchenmeister, C.; Bich, E.; Laesecke, A. Reference correlation of the viscosity of propane. *J. Phys. Chem. Ref. Data* **1998**, *27*, 947−970.

(66) Rainwater, J. C.; Friend, D. G. Second viscosity and thermal conductivity virial coefficients of gases: extension to low reduced temperatures. *Phys. Rev. A* **1987**, *36*, 4062−4066.

(67) Frenkel, M.; Chirico, R. D.; Diky, V. V.; Yan, X.; Dong, Q.; Muzny, C. *ThermoData Engine* (*TDE*), v1.0; National Institute of Standards and Technology: Boulder, CO, 2004.

(68) Friend, D. G.; Rainwater, J. C. Transport properties of a moderately dense gas. *Chem. Phys. Lett.* **1984**, *107*, 590−594.

(69) Reid, R. C.; Prausnitz, J. M.; Poling, B. E. *The Properties of Gases and Liquids*, 4th ed.; McGraw-Hill: New York, 1987.

(70) Huber, M. L.; Laesecke, A.; Perkins, R. Transport properties of *n*-dodecane. *Energy Fuels* **2004**, *18*, 968−975.

(71) Golubev, I. F.; Petrov, V. A. *Trudy GIAP* **1953**, *2*, 5.

(72) Golubev, I. F. *Viscosity of Gases and Gas Mixtures. A Handbook*; Israel Program for Scientific Translations: Jerusalem, 1970.

(73) Assael, M. J.; Polimatidou, S. K. Measurements of the viscosity of alcohols in the temperature range 290−340K at pressures up to 30 MPa. *Int. J. Thermophys.* **1994**, *15*, 95−107.

(74) Bingham, E. C.; White, G. F.; Thomas, A.; Cadwell, J. L. Fluidity and hydration theory. *Z. Phys. Chem.* (*Leipzig*) **1913**, *83*, 641.

(75) Lee, F.-M.; Lahti, L. E.; Stoops, C. E. Solution properties of urea-alcohol-water mixtures. *J. Chem. Eng. Data* **1976**, *21*, 36−40.

(76) Papaioannou, D.; Panayiotou, C. Viscosity of binary mixtures of propylamine with alkanols at moderately high pressures. *J. Chem. Eng. Data* **1995**, *40*, 202−209.

(77) Papanastasiou, G. E.; Ziogas, I. I. Physical behavior of some reaction media. density, viscosity, dielectric constant, and refractive index changes of ethanol-cyclohexane mixtures at several temperatures. *J. Chem. Eng. Data* **1991**, *36*, 46−51.

(78) Phillips, T. W.; Murphy, K. P. Liquid viscosity of halogenated refrigerants. *ASHRAE Trans.* **1970**, *77* (Part II), 146−156.

(79) Boggs, P. T., Byrd, R. H., Rogers, J. E., Schnabel, R. B. *ODRPACK, Software for Orthogonal Distance Regression*; National Institute of Standards and Technology: Gaithersburg, MD, 1992.

(80) Rowley, W. V.; Wilding, J. L.; Oscarson, R. L. *DIADEM, DIPPR Information and Data Evaluation Manager*, v2.7.0; Brigham Young University: Provo, UT, 2004.

(81) Perkins, R. A. Measurement and correlation of the thermal conductivity of isobutane from 114 to 600 K at pressures to 70 MPa. *J. Chem. Eng. Data* **2002**, *47*, 1272−1279.

(82) Perkins, R. A.; Ramires, M. L. V.; Nieto de Castro, C. A.; Cusco, L. Measurement and correlation of the thermal conductivity of butane from 135 to 600 K at pressures to 70 MPa. *J. Chem. Eng. Data* **2002**, *47*, 1263−1271.

(83) Marsh, K. N.; Perkins, R. A.; Ramires, M. L. V. Measurement and correlation of the thermal conductivity of propane from 86 to 600 K at pressures to 70 MPa. *J. Chem. Eng. Data* **2002**, *47*, 932−940.

(84) Naziev, Y. M.; Bashirov, M. M.; Abdulagatov, I. M. High-temperature and high-pressure experimental thermal conductivity for the pure methanol and binary systems methanol + *n*-propanol, methanol+*n*-octanol, and methanol+n-undecanol. *Fluid Phase Equilib.* **2004**, *226*, 221−235.

(85) Raal, J. D.; Rijsdijk, R. L. Measurement of alcohol thermal conductivities using a relative strain-compensated hot-wire method. *J. Chem. Eng. Data* **1981**, *26*, 351−359.

(86) Assael, M. J.; Charitidou, E.; DeCastro, C. A. N. Absolute measurements of the thermal-conductivity of alcohols by the transient hot-wire technique. *Int. J. Thermophys.* **1988**, *9*, 813−824.

(87) Takizawa, S.; Murata, H.; Nagashima, A. Measurement of the thermal conductivity of liquids by transient hot-wire method. *Bull. JSME* **1978**, *21*, 273−278.

(88) Baroncini, C.; Latini, G.; Pierpaoli, P. Thermal conductivity of organic liquid binary mixtures: measurements and prediction method. *Int. J. Thermophys.* **1984**, *5*, 387−401.

(89) Cai, G. Q.; Zong, H. X.; Yu, Q. S.; Lin, R. S. Thermal-conductivity of alcohols with acetonitrile and *N*,*N*-dimethylformamide. *J. Chem. Eng. Data* **1993**, *38*, 332−335.

(90) Tarzimanov, A. A.; Mashirov, V. E. Experimental determination of the coefficient of thermal conductivity of vapors of *n*-alkanes, spirits and acids. *Thermophys. Prop. Matter Subst.* **1974**, *2*, 240−253.

(91) Mukhamedzyanov, I. H.; Mukhamedzyanov, G. H.; Usmanov, A. G. Thermal conductivity of liquid saturated uniaxial alcohols at pressures up to 2500 bar. *Trudy Kazan Inst. Chem. Technol. (Russ.)* **1971**, 57−67.

(92) Rastorguev, Y. L.; Ganiev, Y. A. Thermal conductivity of aqueous solutions of organic liquids. *Russ. J. Phys. Chem.* **1966**, *40*, 869.

(93) Bashirov, M. M. Isobaric heat capacity and thermal diffusivity of alcohols and their binary mixtures. Ph.D. Thesis, ELM, Baku, 2003.

(94) Vargaftik, N. B.; Filippov, L. P.; Tarzimanov, A. A.; Totskii, E. E. *Handbook of Thermal Conductivity of Liquids and Gases*; CRC Press: Boca Raton, FL, 1994.

Received for review January 4, 2005
Revised manuscript received May 24, 2005
Accepted June 7, 2005

IE050010E